Check for updates

Intracellular pathways involved in cell survival are deregulated in mouse and human spinal muscular atrophy motoneurons

Alba Sansa [a], Sandra de la Fuente [a], Joan X. Comella [b], Ana Garcera [a,1], Rosa M. Soler [a,1,*]

[a] *Neuronal Signaling Unit, Experimental Medicine Department, Universitat de Lleida-IRBLleida, Rovira Roure, 80, 25198, Lleida, Spain.*
[b] *CIBERNED & Cell Signaling and Apoptosis Group, Vall d'Hebron Research Institute (VHIR), 08035, Barcelona, Spain.*

ABSTRACT

Spinal Muscular Atrophy (SMA) is a severe neuromuscular disorder caused by loss of the *Survival Motor Neuron 1* gene (*SMN1*). Due to this depletion of the survival motor neuron (SMN) protein, the disease is characterized by the degeneration of spinal cord motoneurons (MNs), progressive muscular atrophy, and weakness. Nevertheless, the ultimate cellular and molecular mechanisms leading to cell loss in SMN-reduced MNs are only partially known. We have investigated the activation of apoptotic and neuronal survival pathways in several models of SMA cells. Even though the antiapoptotic proteins FAIM-L and XIAP were increased in SMA MNs, the apoptosis executioner cleaved-caspase-3 was also elevated in these cells, suggesting the activation of the apoptosis process. Analysis of the survival pathway PI3K/Akt showed that Akt phosphorylation was reduced in SMA MNs and pharmacological inhibition of PI3K diminished SMN and Gemin2 at transcriptional level in control MNs. In contrast, ERK phosphorylation was increased in cultured mouse and human SMA MNs. Our observations suggest that apoptosis is activated in SMA MNs and that Akt phosphorylation reduction may control cell degeneration, thereby regulating the transcription of *Smn* and other genes related to SMN function.

Introduction

Spinal Muscular Atrophy (SMA) is a genetic disorder characterized by the reduction of the ubiquitously expressed protein Survival Motor Neuron (SMN). Among other effects, SMN reduction induces spinal cord motoneuron (MN) degeneration, resulting in muscular atrophy, weakness, and death in the most severe forms of the disease (Lunn and Wang, 2008; Sumner, 2006; Tisdale and Pellizzoni, 2015). SMN is produced by the *SMN1* gene located in the telomeric region of chromosome 5q3 (Lefebvre et al., 1995). In SMA patients, the *SMN1* gene is mutated or deleted and the homologous copy gene *SMN2*, located in the centromeric region of the same chromosome, generates insufficient SMN protein to compensate for *SMN1* loss, due to *SMN2's* defective splicing pattern (Lorson et al., 1999; Monani et al., 1999).

Reduced levels of SMN in spinal cord MNs induce the degeneration of these cells through molecular mechanisms that are not fully understood.

Investigating cell death and intracellular pathways leading to degeneration in SMN-reduced MNs could be relevant to therapeutically prevent or delay SMA disease progression.

Apoptosis is a form of programmed cell death that plays important roles in various physiological and pathological processes. It is an irreversible event that can be initiated by two well-known pathways, intrinsic or extrinsic. Both pathways trigger a cascade of enzymatic activation of caspases (cysteine-aspartic proteases) that destroy the cell by degrading proteins indiscriminately, and it has been proposed that apoptotic pathways play a crucial role in MN loss and SMA development (Maretina et al., 2018).

SMA MN degeneration has been also linked to the upregulation of Fas ligand-mediated apoptosis and to increased caspase-8 and caspase-3 activation (Sareen et al., 2012). Fas, a member of the tumor necrosis factor (TNF) receptor family, is a death receptor that mediates the extrinsic apoptosis of cells. The Fas apoptosis inhibitor molecule (FAIM)

---

is a negative regulator of Fas signaling (Schneider et al., 1999), and the FAIM-L isoform is specifically expressed in neuronal tissues, including spinal cord (Sole et al., 2004). FAIM-L protects neurons from Fas-induced apoptosis through regulating the X-linked inhibitor of apoptosis (XIAP), the most potent caspase inhibitor in vitro (Moubarak et al., 2013; Obexer and Ausserlechner, 2014).

In SMA MNs, expression of the antiapoptotic Bcl-2 and Bcl-xL proteins is reduced (Soler-Botija et al., 2002) and removing Bax-dependent apoptosis has a beneficial effect on SMA phenotype (Tsai et al., 2006). Over-expression of Bcl-xL ameliorates motor functions and prolongs the lifespan in SMA mice (Tsai et al., 2008) and rescues MNs from neurite degeneration and cell death in vitro (Garcera et al., 2011). Loganin, a neuroprotective drug, decreases the number of apoptotic cells and neurite damage in SMA cell model, stimulating the expression of SMN, Gemin2, Akt, and Bcl-2 (Tseng et al., 2016). Changes in the methylation profile for several genes connected with the apoptosis process have been described in SMA patients, such as *OPN3* which is involved in the regulation of apoptosis through the Akt/Bcl-2/Bax pathway (Zheleznyakova et al., 2013). These data suggest apoptosis proteins may participate in *SMN* gene expression, neuronal viability, and neurite outgrowth and could be targets for further research on SMA modifiers, motor function, and survival phenotype.

In the present work, we examined apoptotic and survival pathways in several models of SMA cells, including cultured mouse and human SMA MNs. By western blot analysis we observed an increase of the anti-apoptotic proteins FAIM-L and XIAP in isolated cultured MNs, but a reduction of these proteins in total cell lysates of SMA spinal cords mouse MNs. Reduced levels of FAIM-L and XIAP were also observed in cultured human SMA fibroblasts. Cleaved-caspase-3 and apoptotic nuclei were increased in cultured mice and human SMA MNs, suggesting the activation of the apoptosis pathway in these cells. Finally, we analyzed Akt and ERK phosphorylation profile in SMA cultured MNs. Results showed reduced Akt phosphorylation and increased ERK phosphorylation. Inhibition of PI3K-Akt pathway resulted in SMN protein and *SMN* and *Gemin2* mRNA reduction. Our findings suggest that PI3K/Akt and ERK MAPK pathways are deregulated in SMN-reduced MNs and support the hypothesis that those alterations may regulate apoptosis and SMN level in these cells.

Materials and methods

SMA animals.

Experiments involved the severe SMA mouse model FVB·Cg-Tg (SMN2)[89Ahmb]Smn1[tm1Msd]/J (mutSMA), kindly provided by Dr. Josep E Esquerda and Dr. Jordi Caldero (IRBLleida-Universitat de Lleida). MutSMA mice (Smn^{−/−}; SMN2^{+/+}) were obtained by crossing heterozygous animals. Littermates mutSMA and WT (Smn^{+/+}; SMN2^{+/+}) were used for the experiments.

For MN purification, the heads of 13-day embryos (E13) were snipped for genotyping. The REDExtract-N-Amp Tissue PCR Kit (Sigma) was used for genomic DNA extraction and PCR setup, with the following primers: WT forward 5′-CTCCGGGATATTGGGATTG-3′, SMA reverse 5′-GGTAACGCCAGGGTTTTCC-3′ and WT reverse 5′-TTTCTTCTGG CTGTGCCTTT-3′.

All procedures were done in accordance with the Spanish Council on Animal Care guidelines and approved by the University of Lleida Advisory Committee on Animal Services (CEEA02–01/17).

Spinal cord MN isolation and culture.

MN primary cultures were obtained from the spinal cord of CD1 or SMA mouse embryos at E13 essentially as described (Garcera et al., 2011; Gou-Fabregas et al., 2009). Isolated cells were pooled in culture medium and plated either in laminin-coated four-well tissue culture dishes (Nunc, Thermo Fisher Scientific) for western blot analysis (60,000 cells/well) or using laminin-coated 1-cm^2 glass coverslips placed into the four-well dishes for immunofluorescence experiments (15,000 cells/well). Culture medium was NBM complete (NBMc)–

consisting of neurobasal medium (Gibco, Thermo Fisher Scientific) supplemented with B27 (2% v/v; Gibco), horse serum (2% v/v; Gibco), L-glutamine (0.5 mM; Gibco) and 2-mercaptoethanol (25 μM; Sigma)– and a cocktail of brain-derived neurotrophic factor (BDNF), glial cell line-derived neurotrophic factor (GDNF), cardiotrophin-1 (CT-1) and hepatocyte growth factor (HGF), as follows: 1 ng/ml BDNF, 10 ng/ml GDNF, 10 ng/ml CT-1, and 10 ng/ml HGF (Peprotech). At 24 h after plating, 2 μg/ml of aphidicolin (Sigma) was added to the culture medium and was maintained throughout the experiment.

Human fibroblast cell lines culture.

Human fibroblast cell lines were obtained from the Coriell Institute for Medical Research (Camden, NJ, USA). The Coriell Cell Repository maintains the consent and privacy of the donor samples. All the cell lines and culture protocols in the present study were carried out in accordance with the guidelines approved by institutional review boards at the University of Lleida and IRBLleida research center. Two human fibroblast cell lines from patients with SMA (GM03813, SMA II; and GM09677, SMA I) and one unaffected control (GM03814, Control) were purchased and cultured following the manufacturer instructions. Cells were maintained in Eagle's Minimum Essential Medium (MEM) (Sigma) supplemented with non-inactivated fetal bovine serum (FBS; Gibco) (15% v/v), 0.5 M of L-Glutamine (Gibco), non-essential amino acids (Gibco) (1% v/v), and 20 μg/ml Penicillin-Streptomycin (Gibco). Cells were subcultured every 3–4 days. For western blot analysis, cells were plated at a density of 3000–4000 cells/cm^2 in 35 mm tissue culture dishes and maintained in supplemented MEM. Two days later, total cell lysates were collected and submitted to western blot analysis. For immunofluorescence experiments, 5000 cells/well were plated on 4 well dishes with collagen-coated 1 cm^2 glass coverslips, maintained in the MEM for 24 h and fixed in 4% paraformaldehyde in PBS.

Differentiation of human-induced pluripotent stem cells (iPSCs) to MNs.

The human iPSCs used in the present work were purchased from Coriell Institute for Medical Research. The GM23411*B iPSC cell line (healthy non-fetal tissue) was used as a control (Control) and GM23240*B iPSC cell line (SMA) was from a patient with SMA type II (*SMN2* 2 copies; delta exon7–8 in *SMN1*). Control and SMA cells were differentiated to MNs following the protocol described previously (Du et al., 2015), with minor modifications. Briefly, the human iPSCs were cultured on a layer of irradiated mouse embryonic fibroblasts (MEFs) (Gibco). To generate neuroepithelial (NEP) cells, iPSCs were dissociated with Accutase (Gibco) following manufacturer indications and plated on Geltrex (Gibco)-coated plates in MEF-conditioned medium. Twenty-four hours later, neuroepithelial induction medium (NEPIM: DM/F12:NBM 1:1 supplemented with B27, L-glutamine, and NEAA [all from Gibco]; 0.1 mM ascorbic acid [Sigma]; and 3 μM CHIR99021; 2 μM SB431512; and 2 μM DMH1 [all from Cayman]) was added. Cells were maintained during six days, changing the medium every two days, and dissociated with Accutase to generate motoneuron progenitors (MNP). MNPs were expanded with the same medium (NEPIM) containing 0.1 μM retinoic acid (Sigma), 0.5 μM purmorphamine (Cayman) and 0.5 mM valproic acid (Sigma).

To induce MN differentiation, MNPs were detached with Accutase and cultured in suspension in MN induction medium (NEPIM plus 0.5 μM retinoic acid, 0.1 μM purmorphamine). Medium was changed every two days and after six days the neurospheres were dissociated with Accumax and plated on laminin-coated plates in MN maturation medium (MN induction medium supplemented with 0.1 μM Compound E [Sigma], and 20 ng/ml ciliary neurotrophic factor [CNTF], and 20 ng/ml Insulin-like growth factor 1 [IGF-1], [both from Peprotech]). Dissociated neurospheres were plated in laminin-coated four-well tissue culture dishes (Nunc, Thermo Fisher Scientific) for western blot analysis (60,000 cells/well) or survival and neurite degeneration measurements (15,000 cells/well). For immunofluorescence experiments, cells were plated on 1 cm^2 laminin-coated glass coverslips placed into the four-well dishes (15,000 cells/well).

MN Survival and Neurite Degeneration Analysis.

Dissociated neurospheres were plated in MN maturation medium. Large-phase bright neurons with neurite processes present in photomicrographs of different microscopic areas of culture dishes (four central areas per well, four wells for each condition per experiment) were counted. The number of cells present in each dish on day 0 was considered our initial 100%. Counts were performed in the same microscopic areas as the initial count at days 3, 7, 14, 21 and 28 after plating. Survival was expressed as the percentage of cells counted with respect to the initial value (100%). Morphometric analysis of neurite degeneration was performed as described (Press and Milbrandt, 2008), with modifications. Briefly, human MNs were cultured as described above and phase contrast microscopy images were obtained with a 10× or a 20× lens at 0, 3, 7, 14, 21 and 28 days after plating. A grid was created over each image with NIH ImageJ software (Schneider et al., 2012), using the grid plugin (line area = 50,000). The cell-counting plugin was used to score each neurite. Degenerating and healthy cells were counted in at least 10 high-power fields per image (30–50 neurites) for each well. Four different wells were counted for each condition (with the observer blinded to the condition) and the experiments were repeated at least three times. Neurite segments were considered degenerated if they showed evidence of swelling and/or blebbing.

Western Blot Analysis.

Western blots were performed as previously described (Gou-Fabre-gas et al., 2009). Spinal cord tissue samples were disaggregated using Direct Quant 100ST Buffer (DireCt Quant) and a G50 Tissue Grinder (Coyote Bioscience). Total cell lysates of cultured cells or tissue homogenates were resolved in sodium dodecyl-sulfate polyacrylamide gels and transferred onto polyvinylidene difluoride Immobilon-P transfer membrane filters (Millipore, Billerica, MA, USA) using an Amersham Biosciences semidry Trans-Blot (Buckinghamshire, UK). The membranes were blotted with: anti-SMN (1:5000, Cat. No. 610646, BD Biosciences), anti-FAIM-L (1:2000, Comella J.X.), anti-XIAP (1:5000, Cat. No. 610762, BD Biosciences), anti-cleaved caspase-3 (Asp175, 1:1000, Cat. No. 9661, Cell Signaling Technology), anti-phospho-Akt (Thr 308) (p-Akt, 1:1000, Cat. No. 9275, Cell Signaling Technology), anti-Akt-1 (pan-Akt, 1:10000, Cat. No. SC-1618, Santa Cruz Biotechnology), anti-phospho-p44/42 ERK1/2 Thr202/Tyr204 (p-ERK, 1:15000, Cat. No. 9101, Cell Signaling Technology), or anti-ERK (pan-ERK, 1:5000, Cat. No. 612641, BD Biosciences). To control the specific protein content per lane, membranes were reprobed with monoclonal anti-α-tubulin antibody (1:50000, Cat. No. T5168, Sigma). Blots were developed using Luminata™ Forte Western HRP Substrate (Millipore).

Immunofluorescence.

Lumbar region 1 and lumbar region 2 (L1 and L2) segment of the spinal cords of mutSMA and WT mice was dissected and fixed in 4% paraformaldehyde (Sigma) for 24 h. Cryopreservation with 30% sucrose buffer was done 48 h before mounting segments in tissue freezing medium (TBS, Electron Microscopy Sciences), sectioned at 16-μm thickness in a cryostat (Leica CM3000). Cultured cells were fixed with 4% paraformaldehyde (Sigma) for 10 min and with cold methanol (Sigma) for 10 additional min. Spinal cord slices or cultured cells were permeabilized with 0.2% Triton X-100 and incubated for 2 h with 5% BSA in PBS. Primary antibody (anti-FAIM-L antibody, 1:200, Comella J.X.; anti-XIAP antibody, 1:100, Cat. No. 610762, BD Biosciences; anti-cleaved-caspase-3 [Asp175] antibody, 1:100, Cat. No. 9661, Cell Signaling Technology; anti-HB9 antibody, 1:75, Cat. No. ab92606; anti-ChAT antibody, 1:100, Cat. No. ab18736 [both from Abcam]; or anti-Islet1/2 antibody, 1:50, Cat. No. 39.4D5, Developmental Studies Hybridoma Bank) was diluted in 0.2% Triton-X-100 and incubated overnight with 5% BSA in PBS. After washing, the secondary antibody was added: anti-mouse ALEXA555 antibody, 1:400, Cat. No. A21422; anti-rabbit ALEXA488 antibody, 1:400, Cat. No. A11008 (both from Invitrogen); or anti-sheep ALEXA649 antibody, 1:400, Cat. No. 713–496-147, Jackson ImmunoResearch. Counterstain in spinal cord slices was performed with NeuroTrace 530/615 Red Fluorescent Nissl Stain (1:200, Life

Technologies). Hoechst (1:400, Sigma) staining was performed to identify nuclear localization in cell soma. Samples were mounted using Mowiol (Calbiochem) medium. Microscopy observations were performed in a FV10i Olympus confocal microscope (Tokyo, Japan). Quantification of fluorescence was performed blinded, using the NIH ImageJ software.

RNA Isolation and Quantitative RT-PCR.

For qRT-PCR experiments, isolated CD1 MNs were plated in laminin-coated six-well tissue-culture dishes (Falcon, Corning Incorporated) at a density of 400,000 cells/well. Once the cells were attached, MNs were treated with NBMc medium containing a cocktail of neurotrophic factors with or without 25 μM LY294002 (Calbiochem, Sigma) for 24 h. Total RNA was extracted using the RNeasy® Mini Kit (Qiagen, Hilden, Germany) according to manufacturer instructions. Eighty nanograms of total RNA from each condition were used for each individual qRT-PCR reaction. The assays were performed in a CFX96 Real-Time System (Bio-Rad) using iTaq™ Universal SYBR® Green One-Step Kit from Bio-Rad. For CD1 experiments, Real-Time was performed using mouse SMN-specific primers: SMN exon 1-forward (5′-GATGATTCTGACAT TTGGGATG-3′) and SMN Exon 2-reverse (5′-TGGCTTATCTGGAGTTT-CAGAA-3′) or mouse Gemin2 specific primers: Gemin2 forward (5'-GGGTGAAAGGTTATGTGCTG-3′) and Gemin2 reverse (5'-GTCGGA TTCGTGAATGAGCC-3′) and specific primers of mouse glyceraldehyde-3-phosphate dehydrogenase (GAPDH): forward (5′-TGCACCAC-CAACTGCTTAG-3′) and reverse (5′-GGATGCAGGGATGATGTTC-3′) as internal control. Quantification was completed using Bio-Rad CFX Manager real-time detection system software (version 3.1, Bio-Rad). Relative expression ratios were calculated on the basis of ΔCq values with efficiency correction based on multiple samples.

Statistical analysis

All experiments were performed at least three independent times. Values were expressed as mean ± estimated standard error of the mean (SEM). Statistical analysis was performed using GraphPad Prism, version 8 (GraphPad Software Inc.) Differences between groups were assessed by two-tailed Student t-test. Similar variances between the compared groups were assumed. Values were considered significant when $p < 0.05$.

Results

Changes in antiapoptotic proteins FAIM-L and XIAP in spinal cords and cultured MNs protein extracts from SMA mutant mice.
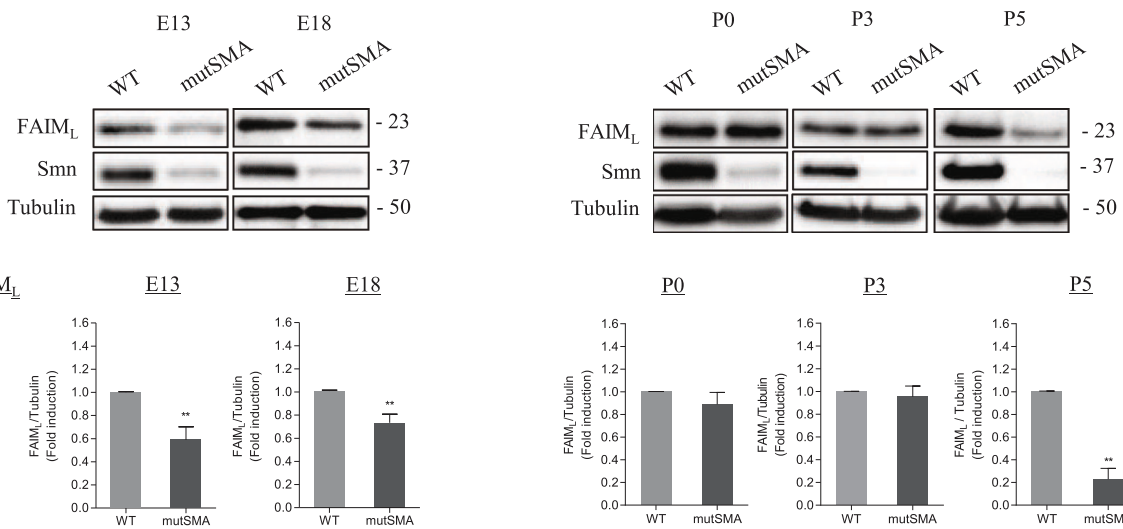
To study the antiapoptotic proteins FAIM-L and XIAP in Smn-reduced tissues, we measured their levels in protein extracts obtained from embryonic and postnatal spinal cords of SMA mice. Wild type (WT) and mutant (mutSMA) mice were genotyped and lumbar regions 1 and 2 (L1 and L2, respectively) of the spinal cords were dissected at the indicated ages. Protein extracts were obtained and submitted to western blot analysis using three antibodies: anti-FAIM-L, anti-XIAP and anti-SMN. As shown in Fig. 1, FAIM-L and XIAP protein levels were significantly reduced in embryonic and late postnatal SMA samples (Fig. 1 and Table 1) compared to the WT control. However, no changes in FAIM-L and XIAP proteins were observed in SMA P0 and P3 samples compared to WT.

To analyze whether FAIM-L and XIAP reduction occurred in spinal cord MNs, these cells were isolated from WT and mutSMA genotyped 13-day mice embryos (E13). MNs were cultured in the presence of neurotrophic factors cocktail for several days (6, 9 and 12 days in vitro, DIV) as indicated, and total cell lysates were obtained. Isolated non-cultured E13 MNs from WT and mutSMA were also submitted to protein extraction (0DIV). Western blot analysis using anti-FAIM-L antibody and anti-XIAP antibody revealed significant increases in mutSMA MNs, compared to the WT control, in FAIM-L protein on all in vitro days measured (6DIV, 9DIV, 12DIV) and in non-cultured cells (0DIV), and in
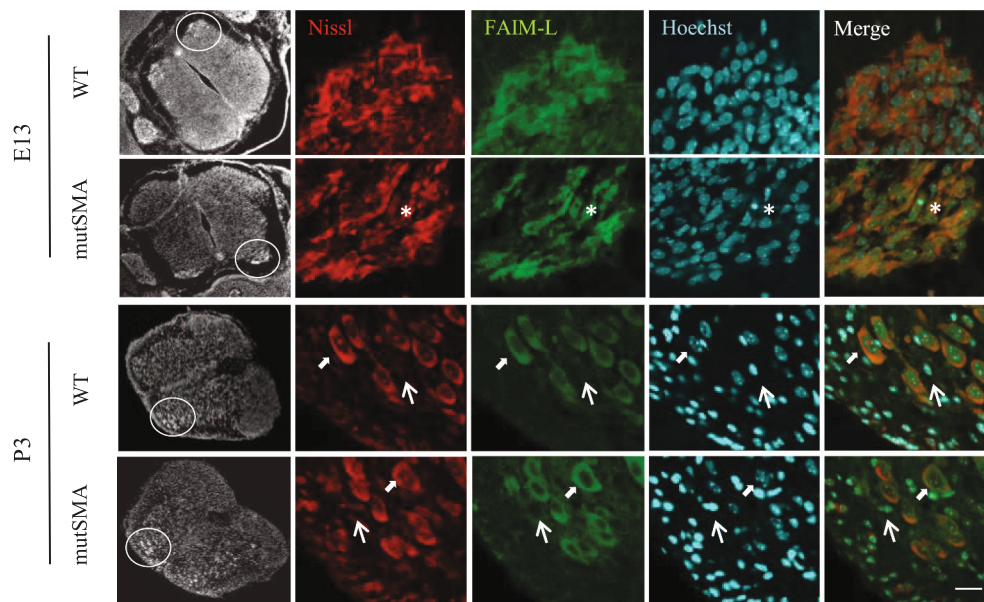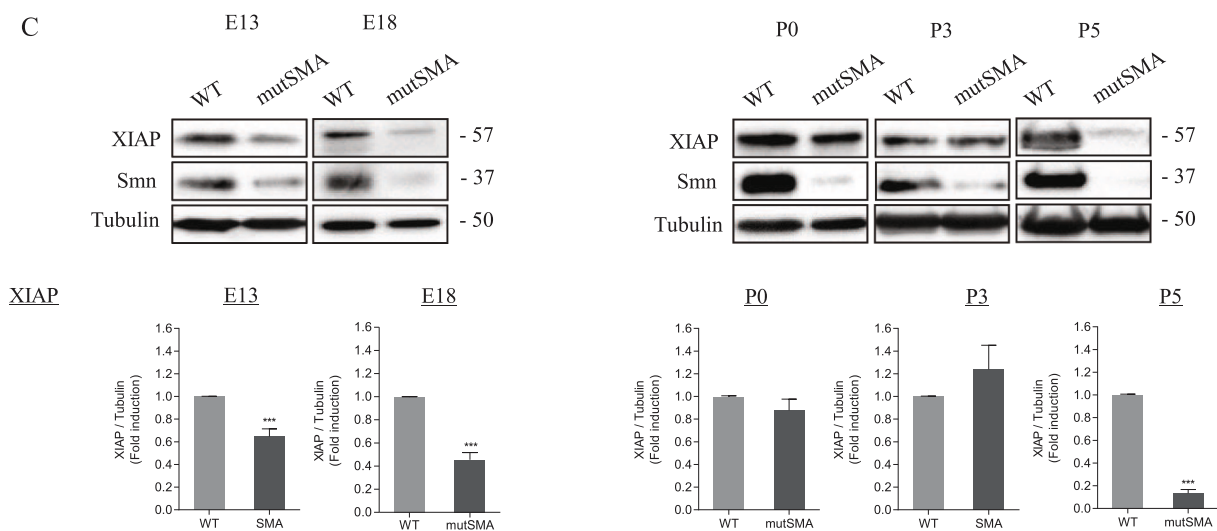
Fig. 1. Antiapoptotic proteins FAIM-L and XIAP levels were reduced in total cell extracts from SMA mice spinal cords. (A) Representative immunofluorescence images of ventral horn spinal cord sections of embryonic 13-day (E13) and postnatal 3-day (P3) from WT and mutSMA mice, using an anti-FAIM-L antibody (green) and Nissl staining (red). Nissl and Hoechst (blue) staining were used to identify MNs soma and nucleus, respectively. Scale bar, 20 μm. White circles indicate ventral MNs pool localization. Bold arrows indicate Nissl and FAIM-L stained cells and thin arrows indicate Nissl and FAIM-L non-stained cells. Asterisk indicates the localization of a cell that appears to be undergoing an apoptotic process. (B and C) Spinal Cords from WT and mutSMA embryonic 13-day (E13), 18-day (E18) and postnatal 0 days (P0), 3-day (P3) and 5-day (P5) mice were dissected and protein extracts were submitted to western blot analysis using anti-FAIM-L antibody (B) or anti-XIAP antibody (C) or anti-SMN antibody (B and C). Membranes were reprobed with anti-α-tubulin antibody. Graph values represent the expression of FAIM-L (B) or XIAP (C) vs α-tubulin and correspond to the quantification of at least three independent experiments ± SEM. Asterisks indicate significant differences using Student *t*-test (**$p < 0.01$; ***$p < 0.001$).

XIAP protein only at 12 DIV and in non-cultured cells (0DIV), as shown in Table 2 and in Fig. 2A and B, respectively. No significant differences in XIAP level were observed in 6DIV and 9DIV WT and mutSMA conditions. Together, these results indicated that levels of FAIM-L and XIAP proteins are reduced in protein extracts of SMA mice spinal cords, but increased in protein extracts of cultured isolated SMA spinal cord MNs, compared to WT control.

XIAP protein level is reduced in human SMA fibroblasts.

The modifications observed in the level of anti-apoptotic proteins in SMA spinal cord and cultured isolated SMA MNs extracts led us to analyze whether XIAP levels were altered in non-neuronal SMA cells. To this end, we cultured human SMA (SMA II and SMA I) and unaffected control fibroblasts. Total protein cell lysates of 2-day cultured cells were submitted to western blot analysis using anti-SMN antibody and anti-XIAP antibody. As expected, results showed that SMN protein level was significantly reduced in cell lysates from SMA fibroblasts (SMA II 0.31 ± 0.03, and SMA I 0.26 ± 0.04, $p < 0.0001$) compared to the clinically unaffected control. In SMN-reduced fibroblasts we observed that XIAP protein level was significantly decreased (SMA II 0.69 ± 0.06, $p = 0.0025$; and SMA I 0.75 ± 0.07, $p = 0.07$) compared to the control condition (Fig. 3). Cultured fibroblasts were fixed and submitted to immunofluorescence protocol using the anti-XIAP antibody and relative fluorescence level of XIAP was measured. As observed in Fig. 3, XIAP fluorescence levels were significantly reduced in SMA fibroblasts (SMA II 8.43 ± 0.68, and SMA I 11.75 ± 0.67, $p < 0.0001$) compared to the control (20.56 ± 1.51). These results together indicate that cultured human SMA fibroblasts show reduced levels of the antiapoptotic protein XIAP.

Cleaved-caspase-3 protein is increased in cultured SMA mice MNs.

Table 1
FAIM-L and XIAP levels in total cell extracts from SMA mice spinal cords

	FAIM-L		XIAP	
Age	*Mean ± SEM*	*p-value*	*Mean ± SEM*	*p-value*
E13	0.59 ± 0.11	0.0067 ¶	0.65 ± 0.07	0.0004 ¶
E18	0.73 ± 0.07	0.0064 ¶	0.45 ± 0.06	0.0007 ¶
P0	0.89 ± 0.10	0.3289	0.88 ± 0.09	0.1474
P3	0.95 ± 0.09	0.6312	1.24 ± 0.21	0.2510
P5	0.23 ± 0.09	0.0013 ¶	0.13 ± 0.03	< 0.0001 ¶

FAIM-L and XIAP levels in protein extracts of lumbar spinal cords fragments from mutSMA compared to the WT controls; ¶ indicate significant differences using Student *t*-test.

Table 2
FAIM-L and XIAP levels in cultured spinal cord MNs from SMA mice

Cultured MNs	FAIM-L		XIAP	
DIV	*Mean ± SEM*	*p-value*	*Mean ± SEM*	*p-value*
0	1.22 ± 0.06	0.0007 ¶	1.5819 ± 0.26	0.0253 ¶
6	1.35 ± 0.10	0.0022 ¶	0.88 ± 0.15	0.4720
9	1.20 ± 0.05	0.0062 ¶	0.78 ± 0.12	0.1620
12	1.34 ± 0.14	0.0293 ¶	1.38 ± 0.13	0.0200 ¶

FAIM-L and XIAP levels in protein extracts of cultured spinal cord isolated MNs from mutSMA mice compared to the WT controls; ¶ indicate significant differences using Student *t*-test.

To further analyze alterations of the apoptotic pathway in Smn-reduced cells, the level of cleaved-caspase-3 and the number of apoptotic nuclei were examined in spinal cord MNs in vitro. To this end, E13 isolated MNs from WT and mutSMA genotyped mice were cultured in the presence of neurotrophic factors cocktail for 6 and 12 days. Protein extracts were obtained and submitted to western blot using an anti-cleaved-caspase-3 antibody. Results showed that the level of cleaved-caspase-3 increased in mutSMA MNs (6DIV 1.57 ± 0.18, $p = 0.0031$; and 12DIV 1.21 ± 0.1, $p = 0.039$) compared to the WT control (Fig. 4A). MNs were also cultured on glass coverslips to implement immunofluorescence experiments. After 6DIV or 12DIV, cells were fixed and immunofluorescence protocol was performed using the anti-cleaved caspase-3 antibody. The percentage of positive cleaved-caspase-3 cells was increased in mutSMA cultured MNs at 6DIV (mutSMA 32.62 ± 4.35) and at 12DIV (mutSMA 69.83 ± 6.48) compared to the WT control (6DIV WT 14.41 ± 0.71, $p = 0.0033$; 12DIV WT 49.71 ± 4.68, $p = 0.0217$, respectively), as shown in Fig. 4B. The percentage of nuclei presenting apoptotic features was evaluated using Hoechst dye. Apoptotic nuclei were significantly increased in 6DIV (26.12 ± 5) and 12DIV (67.45 ± 6.09) mutSMA cells compared to WT at 6DIV (7.99 ± 0.64, $p = 0.0049$) and 12DIV (41.42 ± 4.66, $p = 0.0033$), respectively. These results together indicate that apoptosis is increased in cultured SMA mice MNs.

FAIM-L, XIAP and cleaved-caspase-3 proteins are increased in human differentiated SMA MNs.

To further evaluate the neurodegeneration process occurring in SMN-reduced cells, we next explored survival and neurite degeneration in human MNs differentiated from clinical non-affected (Control) and SMA iPSC. Human SMA and Control iPSC cells were in vitro differentiated to MNs following the protocol described (de la Fuente et al., 2020; Du et al., 2015). Cell survival and neurite degeneration were evaluated at 3, 7, 14, 21 and 28 days after differentiation. The percentage of the surviving cells in the same microscope field was assessed with respect to 100% of day 0 differentiation, and the percentage of degenerating neurites (swelling and blebbing) was considered with respect to the total number of neurites in the microscope field. Results showed that cell survival in the SMA condition was significantly reduced after 14, 21 and 28 days of differentiation compared to Control (3 days: Control 100.03 ± 3.6, SMA 84.24 ± 4.58, $p = 0.053$; 7 days: Control 91.83 ± 4.23, SMA 74.3 ± 5.7, $p = 0.068$; 14 days: Control 81.16 ± 5.2, SMA 43.4 ± 11.9, $p = 0.043$; 21 days: Control 73.56 ± 4.9, SMA 30.86 ± 13.5, $p = 0.041$; and 28 days: Control 67.3 ± 4.1, SMA 26.2 ± 7.9, $p = 0.0098$) (Fig. 5A). When neurite degeneration was evaluated, we observed a significant increase of the percentage of degenerated neurites in differentiated SMA MNs at 7, 14, 21, and 28 days, compared to the Control (3 days: Control 2.65 ± 1.41, SMA 9.29 ± 6.52, $p = 0.37$; 7 days: Control 8.3 ± 3.4, SMA 30.25 ± 6.2, $p = 0.036$; 14 days: Control 13.77 ± 3.6, SMA 51.6 ± 7.0, $p = 0.0086$; 21 days: Control 18.4 ± 4.2, SMA 60.48 ± 7.0, $p = 0.0067$; and 28 days: Control 21.04 ± 5.7, SMA 66.02 ± 8.0, $p = 0.010$) (Fig. 5B).

After 7 days of differentiation, protein extracts from human Control and SMA MNs were obtained and submitted to western blot analysis using anti-SMN, anti-FAIM-L, anti-XIAP, or anti-cleaved caspase-3 antibody. As expected, SMN protein was reduced in SMA (0.32 ± 0.06, $p < 0.0001$) cultures compared to Control (data not shown). When levels of FAIM-L, XIAP, and cleaved-caspase-3 were evaluated, a significant increase of these proteins was observed in SMA-differentiated cells
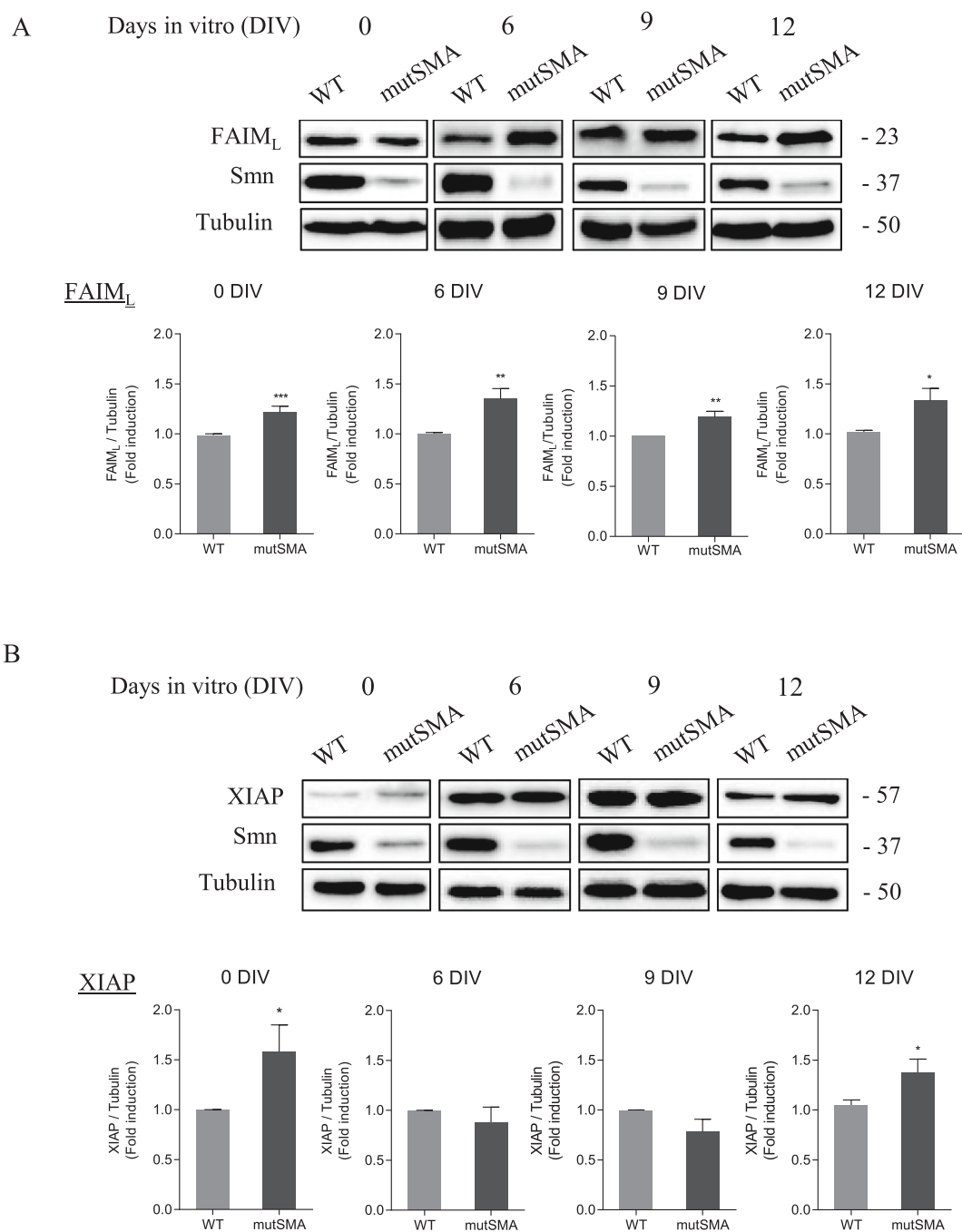
Fig. 2. Antiapoptotic proteins FAIM-L and XIAP levels were increased in cultured spinal cord MNs from SMA mice. Embryonic mouse MNs were isolated from WT or mutSMA genotyped embryos and cultured in the presence of neurotrophic factors cocktail. After 6, 9 and 12 days in vitro (6DIV, 9DIV, 12DIV, respectively) total protein extracts were obtained and submitted to western blot analysis. Protein extracts of non-cultured isolated MNs were also obtained (0DIV) and submitted to western blot analysis. Membranes were probed with anti-FAIM-L antibody (A) or anti-XIAP antibody (B) or anti-SMN antibody (A and B) and were reprobed with an anti-α-tubulin antibody. Graph values represent the expression of FAIM-L or XIAP vs α-tubulin and correspond to the quantification of at least four independent experiments ± SEM. Asterisks indicate significant differences using Student t-test (*$p < 0.05$; **$p < 0.01$; ***$p < 0.001$).

(FAIM-L 1.33 ± 0.38, $p = 0.019$; XIAP 1.37 ± 0.73, $p = 0.034$; cleaved-caspase-3 1.19 ± 0.29, $p = 0.024$), compared to the Control (Fig. 5C). Cleaved-caspase-3 was also analyzed by immunofluorescence. The percentage of cleaved-caspase-3 positive cells was significantly increased in 7-day differentiated SMA human MNs (27.44 ± 2.6) compared to Control (17.3 ± 2.05, $p = 0.012$). Using Hoechst dye, the percentage of MNs displaying nuclei with apoptotic morphology was increased in SMA cultures (34.22 ± 5.73) compared to Control (18.86 ± 2.72, $p = 0.036$) (Fig. 5D). These results together show a deregulated apoptosis pathway in terms of increased anti-apoptotic proteins FAIM-L and XIAP and

increased pro-apoptotic protein cleaved-caspase-3 in human differentiated SMA MNs.

PI3K/Akt and ERK/MAPK intracellular pathways are altered in mouse and human MNs in vitro.

PI3K/Akt and ERK/MAPK are well-known intracellular pathways activated by neurotrophic factors and induce positive effects on spinal cord MNs, such as cell survival (Chao, 2003). To explore whether these pathways are modified in Smn-reduced cells, WT and mutSMA mice MNs were isolated from genotyped E13 embryos. Cells were maintained in the presence of neurotrophic factors during 6 days. Protein extracts
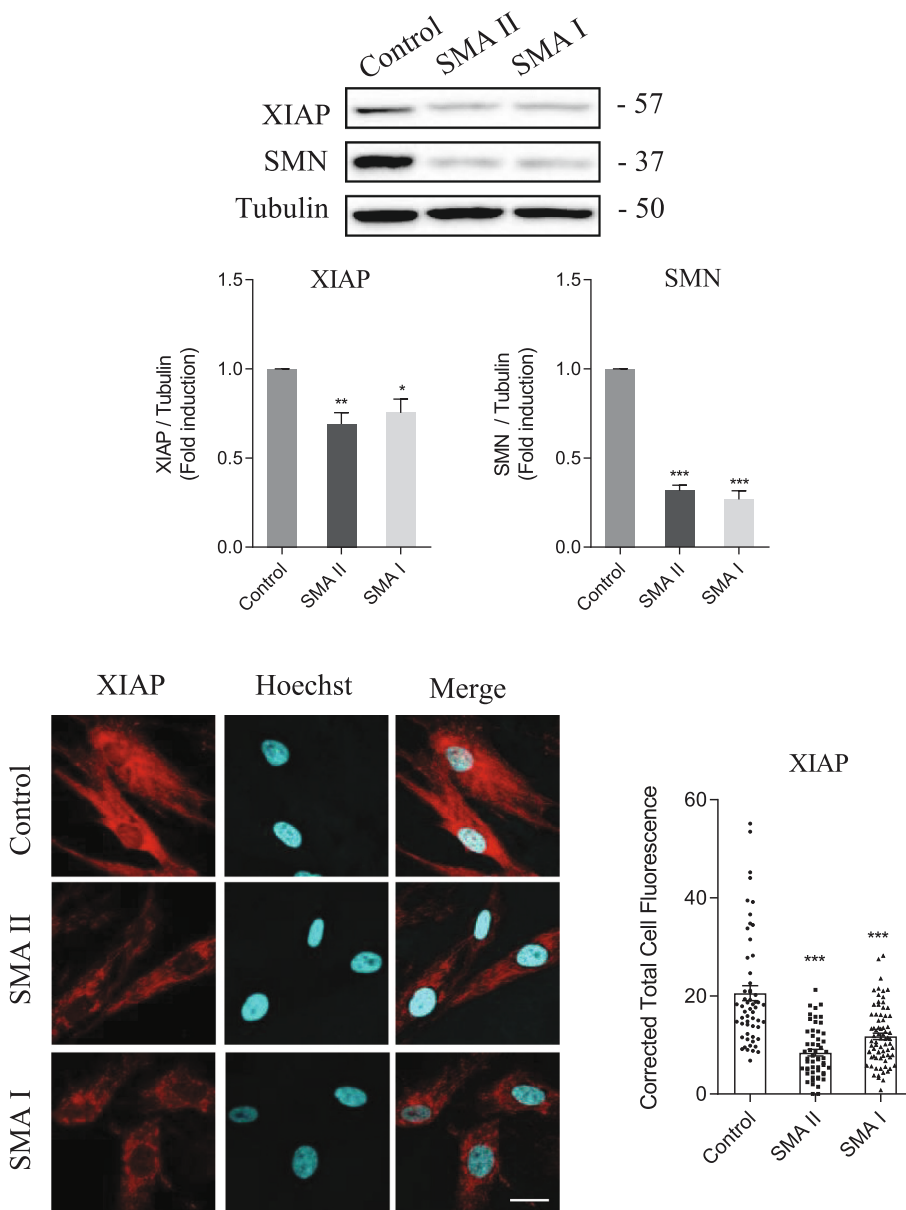
Fig. 3. XIAP protein level was reduced in cultured human SMA fibroblasts. Control (unaffected) and SMA II and SMA I patient fibroblast cell lines were plated in 35 mm culture dishes and maintained in the presence of supplemented MEM. Two days after plating, cell lysates were obtained and submitted to western blot analysis using anti-SMN-antibody or anti-XIAP-antibody. Membranes were reprobed with an anti-α-tubulin antibody. Graph values represent the expression of SMN or XIAP vs α-tubulin and correspond to the quantification of four independent experiments. Asterisks indicate differences using Student *t*-test (*$p < 0.01$; **$p < 0.001$; ***$p < 0.0001$). Representative immunofluorescence images of 2-day cultured fibroblasts in Control and SMAII and SMAI showing XIAP (red) and Hoechst (blue). Hoechst staining was used to identify fibroblast nuclei. Scale bar, 25 μm. Graph represents the mean of relative XIAP fluorescence measured in fibroblasts soma, corresponding to the quantification of at least 25–30 cells per condition from three independent experiments ± SEM. Asterisks indicate significant differences using Student *t*-test (***$p < 0.0001$). Images were acquired with an FV10I confocal microscope (Olympus) using the x60 objective and the same microscopic settings. Images were not submitted to any post-capture manipulation.

were obtained and submitted to western blot analysis using an anti-Akt antibody and anti-phospho-Akt (Thr308) antibody. No significant differences of Akt protein level were observed in WT and mutSMA conditions (Fig. 6A). However, Akt phosphorylation in Thr308 was significantly reduced in mutSMA cells (0.58 ± 0.02, $p < 0.0001$) compared to the WT control (Fig. 6A). To further analyze the role of Akt pathway on Smn regulation we treated the cells with the PI3K inhibitor LY294002. Addition of LY294002 to the culture medium induces apoptotic cell death in cultured CD1 MNs (Dolcet et al., 2001; Soler et al., 1999) and SMA MNs (25 μM LY294002, 24 h treatment: -LY WT $7.8 \pm 1.1\%$ apoptotic nuclei, +LY WT $20.5 \pm 4.4\%$ apoptotic nuclei; -LY mutSMA $8.4 \pm 0.6\%$ apoptotic nuclei, +LY mutSMA $30.1 \pm 2.4\%$ apoptotic nuclei, data not shown). Six-days cultured WT and mutSMA MNs were treated or not with the PI3K inhibitor LY294002 (25 μM). Twenty-four hours later, protein extracts were obtained and submitted to western blot analysis using anti-phospho-Akt (Thr308) antibody, anti-Akt antibody and anti-SMN antibody. When the LY294002 inhibitor was added to the culture medium, Akt phosphorylation was significantly decreased (+LY WT 0.42 ± 0.10, $p = 0.0002$; +LY SMA 0.43 ± 0.11, p = 0.0002) compared to the WT and mutSMA untreated controls (-LY) (data

not shown). When Smn level was analyzed, we observed a significant reduction of this protein in LY294002-treated WT (+LY: 0.57 ± 0.09, $p = 0.0005$) and mutSMA (+LY: 0.42 ± 0.06, $p < 0.0001$) conditions compared to the non-treated controls (-LY WT and –LY mutSMA, respectively) (Fig. 6B). Next, to determine whether the Smn reduction caused by LY294002 treatment was associated with decreased activity of *Smn* gene expression, we quantified *Smn* messenger RNA (mRNA) by quantitative RT-PCR (qRT-PCR). *Gapdh* gene was used as a control. Embryonic (E13) spinal cord isolated CD1 mice MNs were plated and cultured in the presence of the neurotrophic factors cocktail with or without 25 μM LY294002. After 24 h, total RNA was extracted and reverse-transcribed to cDNA, used as a template to quantify *Smn* transcript level. LY294002 addition was related to a reduction in Smn mRNA expression (0.58 ± 0.034, $p < 0.0001$) compared with control non-treated condition, showing that PI3K inhibition regulates Smn at transcriptional level (Fig. 6C). We also quantified *Gemin2* mRNA, which is part of a protein complex with SMN in the axonal compartment (Zhang et al., 2006). Results indicated that *Gemin2* mRNA expression (0.65 ± 0.029, $p < 0.0001$) was reduced in LY294002 treated cells compared to the non-treated control (Fig. 6C).
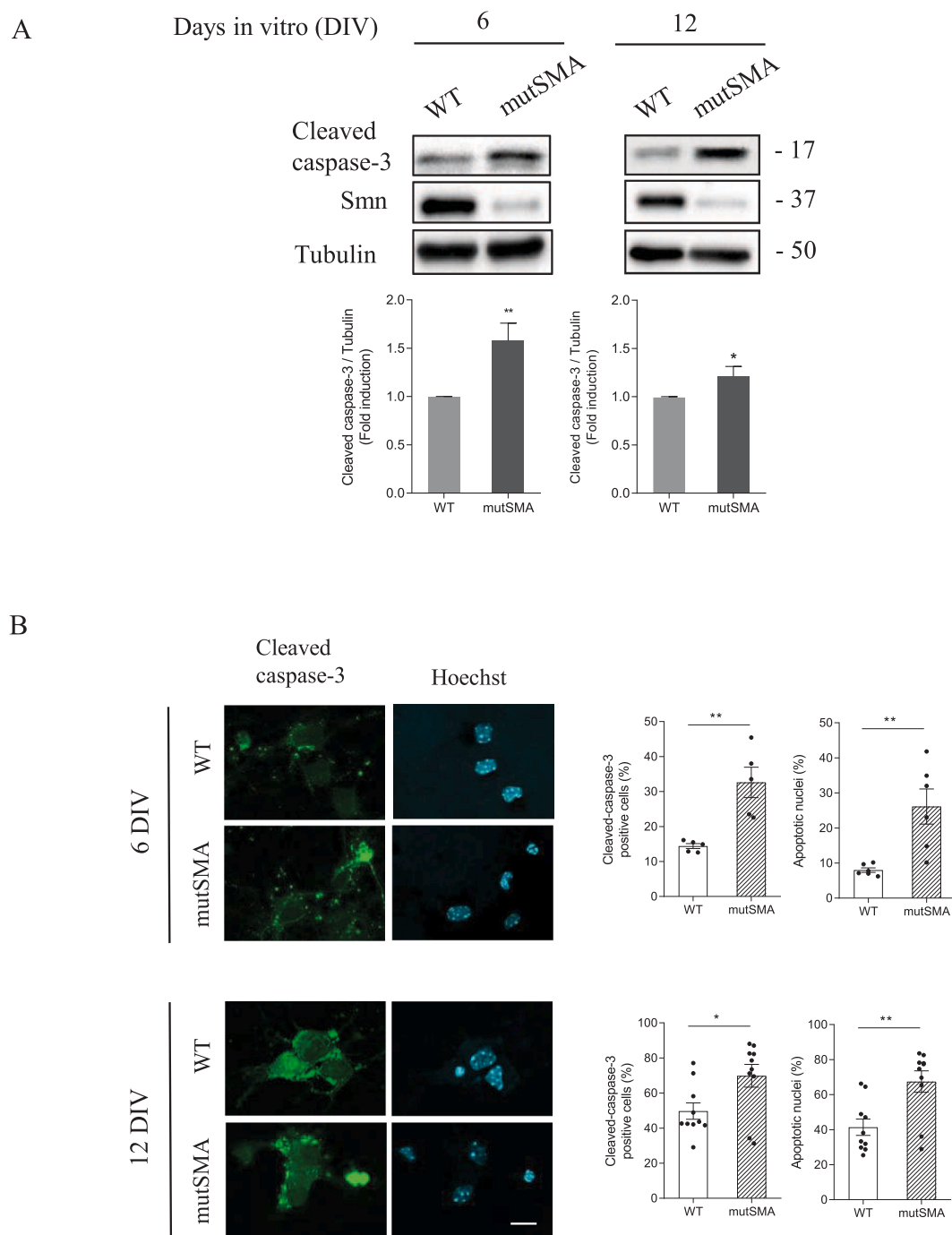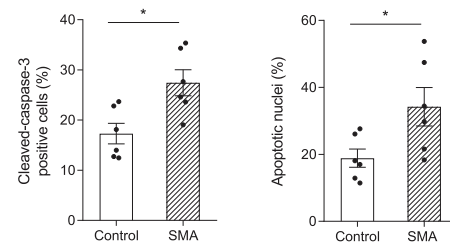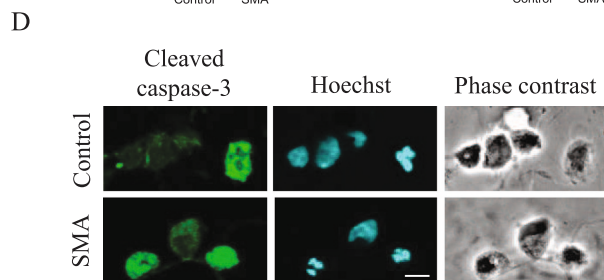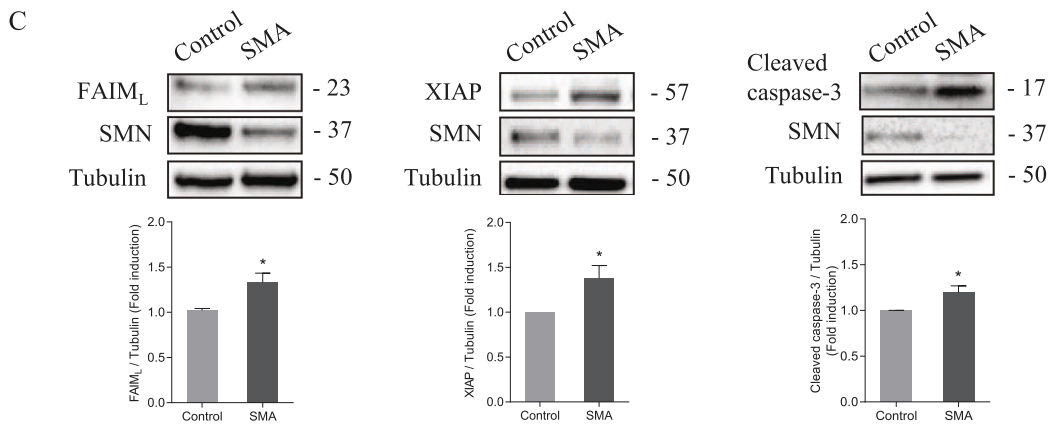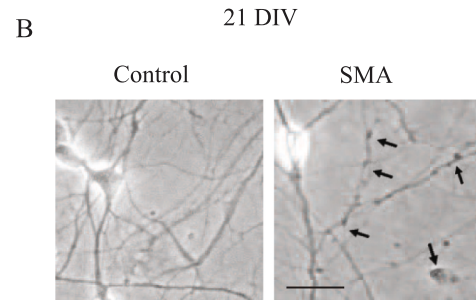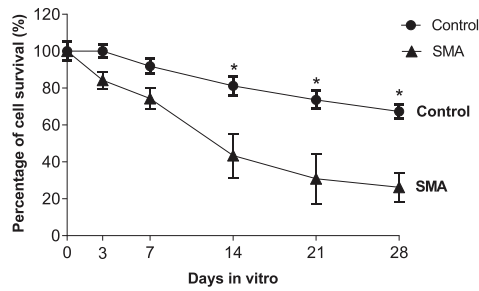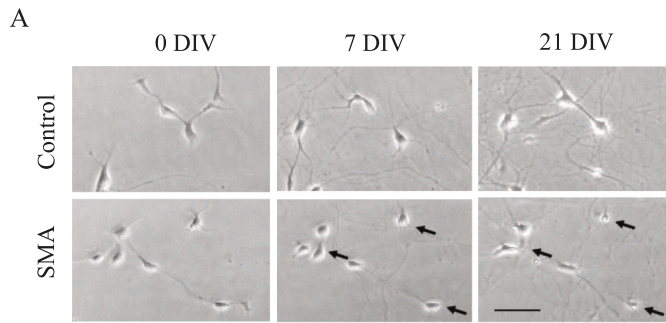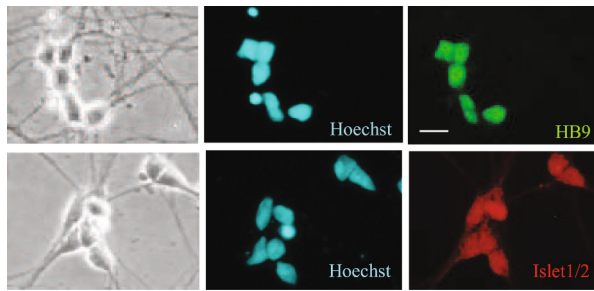
Fig. 4. Cleaved-caspase-3 level was increased in SMA MNs. (A) WT and mutSMA spinal cord MNs were isolated and cultured in the presence of a neurotrophic factors cocktail. After 6 and 12 days in vitro (6DIV and 12DIV, respectively) protein extracts were obtained and submitted to western blot analysis using an anti-cleaved-caspase-3 antibody or anti-Smn antibody. Membranes were reprobed with an anti-α-tubulin antibody, used as a loading control. Graphs represent the expression of cleaved-caspase-3 corresponding to the quantification of at least six independent experiments ± SEM. Asterisks indicate differences using Student t-test (*$p < 0.05$; **$p < 0.005$). (B) Representative confocal images of immunostained 6DIV and 12DIV MNs using an anti-cleaved-caspase-3 antibody. Hoechst (blue) dye was used to identify apoptotic and non-apoptotic nuclei. Graphs represent the percentage of cleaved-caspase-3 positive cells or the percentage of nuclei showing apoptotic morphology, corresponding to the quantification of at least four independent experiments (~ 200 cells/well, 1–2 well/experiment) ± SEM. Asterisks indicate differences using Student t-test (*$p < 0.05$; **$p < 0.005$). Scale bar, 15 μm.

To further evaluate changes of survival intracellular pathways in SMN-reduced cells, we explored protein level and phosphorylation of Akt and ERK in human differentiated MNs. Human SMA and control iPSC were in vitro differentiated to MN. Seven days after differentiation, total cells lysates were collected and analyzed by western blot using anti-phospho-Akt (Thr308) antibody, anti-Akt antibody, anti-phospho-ERK antibody and anti-ERK antibody. Akt protein level (0.82 ± 0.04, $p =$

0.0003) and Thr308 phosphorylation (0.64 ± 0.09, $p = 0.0058$) were observed to be significantly reduced in human SMA cultured MNs compared to the control condition (Fig. 7A). In western blot analysis, no changes in total ERK protein level were found in SMA compared to control samples. However, measures of phospho-ERK level displayed significant differences, with increased ERK phosphorylation in SMA (4.16 ± 1.36, $p = 0.043$) compared to the control condition. The same
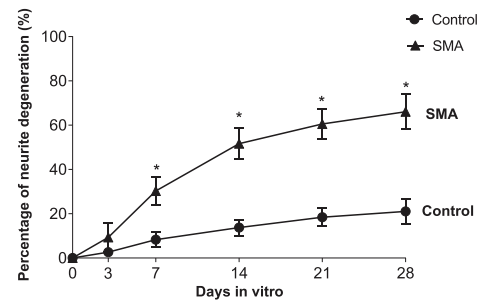
(caption on next page)

Fig. 5. Cell death, neurite degeneration and cleaved-caspase-3 protein level were increased in human SMA iPSC differentiated MNs. Representative phase contrast and immunofluorescence images of 7-day differentiated Control and SMA human MNs, showing the MN markers HB9 (green), Islet ½ (red left section) and ChAT (red right section). Hoechst (blue) staining was used to identify MN nuclei. Scale bar, 30 μm (left) and 15 μm (right). (A) Representative images of the same microscopic field of Control and SMA human MNs differentiated for 0, 7, and 21 days (0DIV, 7DIV, 21DIV, respectively). Arrows indicate degeneration of MN soma. Graph values are the mean of the percentage of cell survival for each condition of 12 wells from three independent experiments ± SEM. (B) Representative images of Control and SMA human MNs differentiated for 21 days (21DIV). Arrows indicate degeneration of neurites. Graph values are the mean of the percentage of degenerating neurites for each condition of 12 wells from three independent experiments ± SEM. Asterisks indicate differences using Multiple t-test (*$p < 0.05$). Scale bar, 50 μm (in A) and 30 μm (in B). (C) Protein extracts of 7-day differentiated Control and SMA human MNs were submitted to western blot analysis using anti-FAIM-L antibody or anti-XIAP antibody or anti-cleaved-caspase-3 antibody or anti-SMN antibody. Membranes were reprobed with an anti-α-tubulin antibody, used as a loading control. Graphs represent the expression of FAIM-L, XIAP or cleaved-caspase-3, corresponding to the quantification of at least four independent experiments ± SEM. Asterisks indicate differences using Student t-test (*$p < 0.05$). (D) Representative immunofluorescence confocal images of 7-day differentiated human MNs using an anti-cleaved-caspase-3 antibody. Hoechst dye was used to identify apoptotic and non-apoptotic nuclei. Graphs represent the percentage of cleaved-caspase-3 positive MNs or the percentage of nuclei showing apoptotic morphology, corresponding to the quantification of three independent experiments ± SEM. Asterisks indicate differences using Student t-test (*$p < 0.05$). Scale bar, 15 μm.

profile of ERK protein level and phosphorylation was observed in cultured WT and mutSMA mice MNs (p-ERK/pan-ERK in mouse mutSMA cultures 2.12 ± 0.3 fold-induction, $p = 0.0036$, compared to the WT control) (data not shown).

Discussion

The deregulation in SMA disease of intracellular processes involved in MN homeostasis and survival has been described, but the cellular
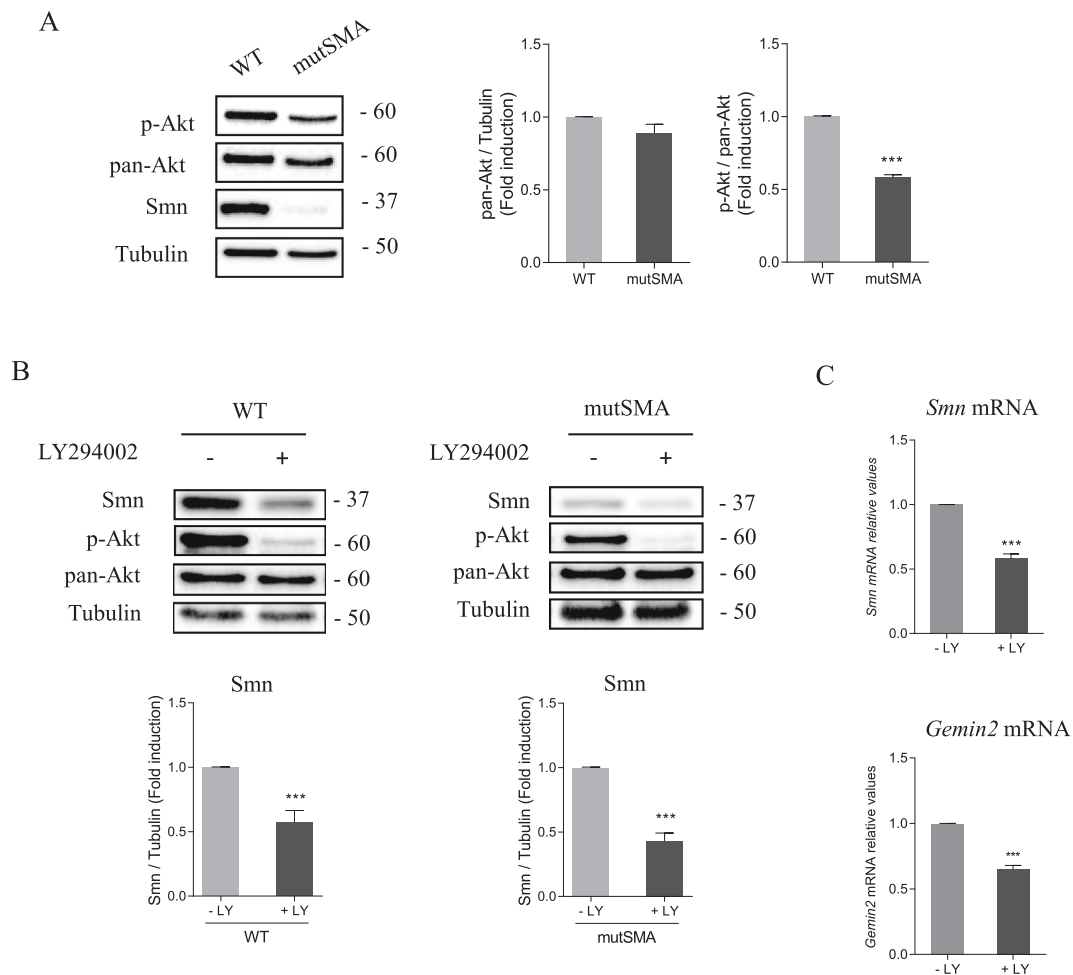

Fig. 6. PI3K/AKT pathway regulates Smn at transcriptional level. WT and mutSMA spinal cord MNs were isolated and cultured in the presence of a neurotrophic factors cocktail. (A) Six days after plating, protein extracts were obtained and submitted to western blot analysis using anti-phospho-Akt (Thr308) antibody and anti-SMN antibody. Membranes were stripped and reprobed with an anti-Akt antibody or reprobed with an anti-α-tubulin antibody. Graphs represent the expression of Akt (left graph) or the expression of phospho-Akt versus Akt and indicate fold-reduction contrasted with WT condition (right graph) from at least three independent experiments ± SEM. Asterisks indicate differences using Student t-test (***$p < 0.0001$). (B) After 6 days, in vitro cells were washed and treated with 25 μM LY294002 or left untreated. Twenty-four hours later, protein extracts were obtained and submitted to western blot analysis using anti-phospho-Akt (Thr308) antibody and anti-SMN antibody. Membranes were stripped with an anti-Akt antibody or reprobed with an anti-α-tubulin antibody. Graphs represent the expression of Smn vs α-tubulin, corresponding to the quantification of three independent experiments ± SEM. Asterisks indicate differences using Student t-test (***$p < 0.0001$). (C) Total RNA was extracted from 25 μM LY294002-treated (+LY) or non-treated (-LY) CD1 MN cultures and reverse transcribed to cDNA. *Gapdh* gene was used as control. Graph values are the mean of *Smn* gene or *Gemin2* gene expression from three independent experiments ± SEM. Asterisks indicate significant differences using Student t-test (***$p < 0.0001$).
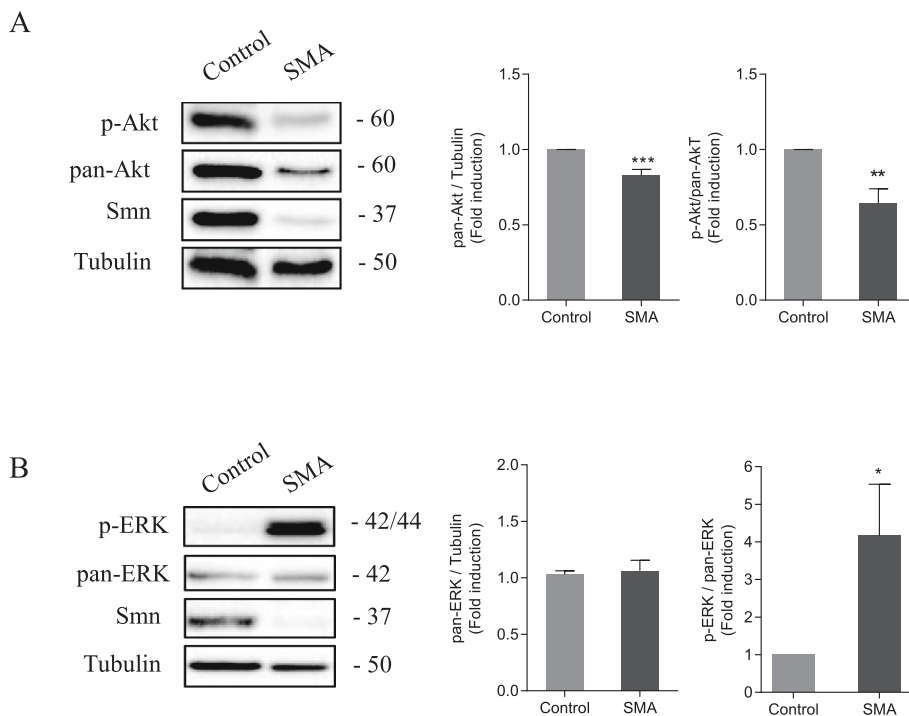
Fig. 7. Changes of Akt and ERK phosphorylation in protein extracts of human differentiated MNs. Control and SMA human iPSCs were submitted to MN differentiation protocol. Total cell lysates of 7-day differentiated MNs were submitted to western blot analysis using anti-phospho-Akt (Thr308) antibody (A), anti-phospho-p44/42 MAPK (ERK1/2) (Thr202/Tyr204) antibody (B) and anti-SMN antibody (A and B). Membranes were stripped with anti-Akt antibody or anti-ERK antibody, or reprobed with an anti-α-tubulin antibody. Graphs represent the expression of Akt vs α-tubulin (A, left) or phospho-Akt vs Akt (A, right) and indicate fold-induction compared to Control condition; or ERK vs α-tubulin (B, left) or phospho-ERK vs ERK (B, right) and fold-induction compared to Control (A right) and corresponding to the quantification of three independent experiments ± SEM. Asterisks indicate differences using Student t-test (*$p < 0.05$, **$p < 0.01$, ***$p < 0.001$).

mechanisms leading to degeneration of SMN-reduced spinal cord MNs are not completely understood. One of these processes is apoptotic cell death. In the present study we analyzed apoptosis and survival pathways in several models of SMA cells, including human differentiated SMA MNs. Our results suggest that apoptosis regulators and PI3K/Akt and ERK MAPK intracellular pathways are compromised in SMA cells. Additionally, we described PI3K/Akt inhibition as regulating *Smn* and *Gemin2* at transcriptional level in cultured MNs.

FAIM-L (Fas apoptosis inhibitory molecule) has been identified as an inhibitor of Fas signaling and apoptosis through the regulation of XIAP (X-linked inhibitor of apoptosis) (Moubarak et al., 2013). Deregulation of XIAP has been described in some neuropathologies (e.g., Alzheimer's disease, Huntington disease, amyotrophic lateral sclerosis, and axotomy) (Christie et al., 2007; Goffredo et al., 2005; Guégan et al., 2001; Kügler et al., 2000) and FAIM-L reduction is associated with the progression of Alzheimer's disease (Carriba et al., 2015; Huo et al., 2019). Given the involvement of these proteins in neurodegenerative processes where neuronal cell survival plays a critical role, it is not difficult to speculate that FAIM and XIAP may be involved in SMA disease. Western blot analysis of spinal cord protein extracts from SMA mice showed decreased levels of FAIM-L and XIAP at embryonic period and at postnatal end-stage of the disease. Reduced levels of these proteins may be related to an increase in apoptotic cell death (Moubarak et al., 2013). Nevertheless, the level of FAIM-L and XIAP did not change or were increased in SMA cultured MNs. Similarly, protein extracts of differentiated human MNs showed increased FAIM-L and XIAP. FAIM-L regulates XIAP by inhibiting its auto-ubiquitination and maintaining its stability. In fact, FAIM-L could sustain endogenous levels of XIAP in murine cortical neurons (Moubarak et al., 2013). The presence of FAIM-L can interact with de baculovirus IAP repeat (BIR)2 domain of XIAP preventing its degradation and protein level reduction (Moubarak et al., 2013). Our results showed increased FAIM-L protein level in cultured SMA MNs suggesting that FAIM-L can be regulating XIAP stability in these cells resulting in an elevation or non-reduction of XIAP protein level.

Spinal cord lysates include protein extracts of MNs and their surrounding cells, such as interneurons and glial cells. Therefore, FAIM-L and XIAP reduction indicates a generalized decrease of these proteins in the spinal cord of SMA mice. When XIAP protein was examined in cultured human SMA fibroblasts, results showed reduced levels of this protein. These results together suggest that in SMA condition the anti-apoptotic proteins FAIM-L and XIAP are differentially regulated in MNs and non-neuronal cells. This observation may be related to the hypothetic role of FAIM-L and XIAP expression as indicators of disease evolution or progression in SMA, as has been suggested in other neurodegenerative disorders (Carriba and Comella, 2015). In mice and human SMA MNs, we observed apoptotic features even when FAIM-L and XIAP levels increased. Moreover, human differentiated MNs showed increased neurite degeneration and cell death, suggesting that FAIM-L and XIAP expression did not prevent MN degeneration. The activation of PI3K/Akt and/or NFkappaB pathways by neurotrophic factors mediates in vitro MN survival and their inhibition causes apoptotic cell death (Dolcet et al., 2001; Mincheva et al., 2011; Soler et al., 1999). Akt phosphorylation (Fig. 6 and Fig. 7) and p65 (RelA) phosphorylation (Arumugam et al., 2018) are reduced in cultured SMA MNs. These observations indicate that two of the main MN survival pathways are compromised in SMA cells and it may initiate the apoptotic signal that could not be counteracted by the antiapoptotic proteins FAIM-L and XIAP. Thereby, FAIM-L and XIAP increase may reflect a cellular reaction to prevent apoptosis induced by SMN reduction and, as a consequence, to slow down the process. In Drosophila S2 cell line, SMN deficiency activates caspase-dependent apoptosis, which can be prevented by caspase inhibitors (Ilangovan et al., 2003). An increase in Fas ligand-mediated apoptosis and increased caspase-8 and caspase-3 activation in human differentiated SMA MNs has also been described (Sareen et al., 2012). Bcl-2 family proteins known to be key regulators of apoptosis are reduced in MNs of SMA fetuses, suggesting an enhanced apoptosis cell death in these cells (Soler-Botija et al., 2002). In SMA pathogenesis, Bcl-2 regulating protein WT-1 is expressed at lower levels in SMA mouse model (Anderson et al., 2003) and overexpression of Bcl-xL ameliorated motor functions and prolonged lifespan in SMA mice (Tsai et al., 2008) and rescued mouse MNs from neurite degeneration and cell death in vitro (Garcera et al., 2011). Therefore, our present results support the hypothesis that the apoptotic process is activated in SMA MNs.

Nonetheless, other cellular mechanisms may also contribute to MN

degeneration. Here, we show that the survival intracellular pathways PI3K/Akt and ERK MAPK are deregulated in SMA MNs. Akt phosphorylation is reduced in mice and human cultured SMA MNs, and ERK phosphorylation in increased in these cells. In this context, previously published results demonstrated that PI3K/Akt and ERK MAPK pathways activation profile are affected in SMA tissues (Biondi et al., 2015). Biondi and collaborators showed reduced Akt phosphorylation and increased ERK phosphorylation in SMA spinal cord and tibialis muscle protein extracts. The authors postulated that Akt activation increases SMN at transcriptional level through the Akt/CREB pathway, and ERK activation may reduce SMN transcription through the ERK/Elk-1 pathway. In accordance with these previous studies, our results show that PI3K/Akt pathway inhibition reduced Smn at transcriptional level in cultured MNs. Therefore, decreased Akt phosphorylation observed in SMA MNs may contribute to the reduction of SMN level in these cells. We also describe an increase of ERK phosphorylation in SMA MNs which, based on a previous hypothesis, may aggravate SMN protein reduction in these cells. Thus, the changes in the phosphorylation profile observed in MNs may contribute to exacerbate SMA disease progression. On the other hand, it is known that ERK activation by neurotrophic factors increases FAIM-L expression in neuronal PC12 cells, protecting them from Fas-induced apoptosis by regulating XIAP (Moubarak et al., 2013; Segura et al., 2007). Therefore, the observed increase of FAIM-L in SMA MNs may be the consequence of a rise in ERK activation in these cells. Nevertheless, the FAIM-L and XIAP increase in SMN-reduced MNs was not sufficient to prevent caspase-3 activation and apoptotic cell death.

PI3K/AKT inhibition by LY294002 also reduced *Gemin2* mRNA in mouse cultured MNs. Gemin2 is associated in a protein complex with SMN, Gemin3, and hnRNPR in the axonal compartment of MNs and is localized in granules that are actively transported into neuronal processes and growth cones. It has been suggested that the absence of spliceosomal Sm proteins in this complex contributes to a distinct function of SMN in the axon from that in the neural cell body (Talbot and Davies, 2008; Zhang et al., 2006; Zhang et al., 2008). Our present results suggest that reduced PI3K/Akt pathway activation observed in SMA MNs may contribute to the aforementioned deficiency of SMN and Gemin2 proteins in the axonal complexes and its effect on their specific function in these cells.

In conclusion, the present study found reduction of Akt phosphorylation and increase of ERK phosphorylation and cleaved-caspase-3 in SMN-reduced mouse and human MNs. These changes in intracellular pathways may be related to the increase of FAIM-L and XIAP antiapoptotic proteins, but also to reduced SMN and Gemin2 protein levels, which can contribute to MN degeneration. Regulating the activity of these pathways together with the analysis of new SMA modifiers belonging to other intracellular pathways which contribute differently to disease progression may lead to the discovery of new SMA treatment strategies.

Author statement.

Alba Sansa: Conceptualization, Investigation, Formal analysis, Writing-Original Draft, Visualization.

Sandra de la Fuente: Investigation, Formal Analysis, Validation, Conceptualization.

Joan X Comella: Resources, Conceptualization, Funding acquisition.

Ana Garcera: Supervision, Methodology Development, Project administration.

Rosa M Soler: Conceptualization, Supervision, Writing original draft and reviewing, Visualization, Funding acquisition.

References

Anderson, K., Potter, A., Baban, D., Davies, K.E., 2003. Protein expression changes in spinal muscular atrophy revealed with a novel antibody array technology. Brain 126, 2052–2064.

Arumugam, S., Mincheva-Tasheva, S., Periyakaruppiah, A., de la Fuente, S., Soler, R.M., Garcera, A., 2018. Regulation of survival motor neuron protein by the nuclear factor-kappa B pathway in mouse spinal cord Motoneurons. Mol. Neurobiol. 55, 5019–5030.

Biondi, O., Branchu, J., Ben Salah, A., Houdebine, L., Bertin, L., Chali, F., Desseille, C., Weill, L., Sanchez, G., Lancelin, C., Aïd, S., Lopes, P., Pariset, C., Lécolle, S., Côté, J., Holzenberger, M., Chanoine, C., Massaad, C., Charbonnier, F., 2015. IGF-1R reduction triggers Neuroprotective signaling pathways in spinal muscular atrophy mice. J. Neurosci. 35, 12063–12079.

Carriba, P., Comella, J.X., 2015. Neurodegeneration and neuroinflammation: two processes, one target. Neural Regen. Res. 10, 1581–1583.

Carriba, P., Jimenez, S., Navarro, V., Moreno-Gonzalez, I., Barneda-Zahonero, B., Moubarak, R.S., Lopez-Soriano, J., Gutierrez, A., Vitorica, J., Comella, J.X., 2015. Amyloid-β reduces the expression of neuronal FAIM-L, thereby shifting the inflammatory response mediated by TNFα from neuronal protection to death. Cell Death Dis. 6, e1639.

Chao, M.V., 2003. Neurotrophins and their receptors: a convergence point for many signalling pathways. Nat. Rev. Neurosci. 4, 299–309.

Christie, L.A., Su, J.H., Tu, C.H., Dick, M.C., Zhou, J., Cotman, C.W., 2007. Differential regulation of inhibitors of apoptosis proteins in Alzheimer's disease brains. Neurobiol. Dis. 26, 165–173.

de la Fuente, S., Sansa, A., Hidalgo, I., Vivancos, N., Romero-Guevara, R., Garcera, A., Soler, R.M., 2020. Calpain system is altered in survival motor neuron-reduced cells from in vitro and in vivo spinal muscular atrophy models. Cell Death Dis. 11, 487.

Dolcet, X., Soler, R.M., Gould, T.W., Egea, J., Oppenheim, R.W., Comella, J.X., 2001. Cytokines promote motoneuron survival through the Janus kinase-dependent activation of the phosphatidylinositol 3-kinase pathway. Mol. Cell. Neurosci. 18, 619–631.

Du, Z.W., Chen, H., Liu, H., Lu, J., Qian, K., Huang, C.L., Zhong, X., Fan, F., Zhang, S.C., 2015. Generation and expansion of highly pure motor neuron progenitors from human pluripotent stem cells. Nat. Commun. 6, 6626.

Garcera, A., Mincheva, S., Gou-Fabregas, M., Caraballo-Miralles, V., Llado, J., Comella, J.X., Soler, R.M., 2011. A new model to study spinal muscular atrophy: Neurite degeneration and cell death is counteracted by BCL-X-L overexpression in motoneurons. Neurobiol. Dis. 42, 415–426.

Goffredo, D., Rigamonti, D., Zuccato, C., Tartari, M., Valenza, M., Cattaneo, E., 2005. Prevention of cytosolic IAPs degradation: a potential pharmacological target in Huntington's disease. Pharmacol. Res. 52, 140–150.

Gou-Fabregas, M., Garcera, A., Mincheva, S., Perez-Garcia, M.J., Comella, J.X., Soler, R. M., 2009. Specific vulnerability of mouse spinal cord motoneurons to membrane depolarization. J. Neurochem. 110, 1842–1854.

Guégan, C., Vila, M., Rosoklija, G., Hays, A.P., Przedborski, S., 2001. Recruitment of the mitochondrial-dependent apoptotic pathway in amyotrophic lateral sclerosis. J. Neurosci. 21, 6569–6576.

Huo, J., Xu, S., Lam, K.P., 2019. FAIM: an antagonist of Fas-killing and beyond. Cells 8.

Ilangovan, R., Marshall, W.L., Hua, Y., Zhou, J., 2003. Inhibition of apoptosis by Z-VAD-fmk in SMN-depleted S2 cells. J. Biol. Chem. 278, 30993–30999.

Kügler, S., Straten, G., Kreppel, F., Isenmann, S., Liston, P., Bähr, M., 2000. The X-linked inhibitor of apoptosis (XIAP) prevents cell death in axotomized CNS neurons in vivo. Cell Death Differ. 7, 815–824.

Lefebvre, S., Burglen, L., Reboullet, S., Clermont, O., Burlet, P., Viollet, L., Benichou, B., Cruaud, C., Millasseau, P., Zeviani, M., et al., 1995. Identification and characterization of a spinal muscular atrophy-determining gene. Cell 80, 155–165.

Lorson, C.L., Hahnen, E., Androphy, E.J., Wirth, B., 1999. A single nucleotide in the SMN gene regulates splicing and is responsible for spinal muscular atrophy. Proc. Natl. Acad. Sci. U. S. A. 96, 6307–6311.

Lunn, M.R., Wang, C.H., 2008. Spinal muscular atrophy. Lancet 371, 2120–2133.

Maretina, M.A., Zheleznyakova, G.Y., Lanko, K.M., Egorova, A.A., Baranov, V.S., Kiselev, A.V., 2018. Molecular factors involved in spinal muscular atrophy pathways as possible disease-modifying candidates. Curr Genomics 19, 339–355.

Mincheva, S., Garcera, A., Gou-Fabregas, M., Encinas, M., Dolcet, X., Soler, R.M., 2011. The canonical nuclear factor-kappa B pathway regulates cell survival in a developmental model of spinal cord Motoneurons. J. Neurosci. 31, 6493–6503.

Monani, U.R., Lorson, C.L., Parsons, D.W., Prior, T.W., Androphy, E.J., Burghes, A.H., McPherson, J.D., 1999. A single nucleotide difference that alters splicing patterns distinguishes the SMA gene SMN1 from the copy gene SMN2. Hum. Mol. Genet. 8, 1177–1183.

Moubarak, R.S., Planells-Ferrer, L., Urresti, J., Reix, S., Segura, M.F., Carriba, P., Marqués-Fernàndez, F., Sole, C., Llecha-Cano, N., Lopez-Soriano, J., Sanchis, D., Yuste, V.J., Comella, J.X., 2013. FAIM-L is an IAP-binding protein that inhibits XIAP

ubiquitinylation and protects from Fas-induced apoptosis. J. Neurosci. 33, 19262–19275.

Obexer, P., Ausserlechner, M.J., 2014. X-linked inhibitor of apoptosis protein - a critical death resistance regulator and therapeutic target for personalized cancer therapy. Front. Oncol. 4, 197.

Press, C., Milbrandt, J., 2008. Nmnat delays axonal degeneration caused by mitochondrial and oxidative stress. J. Neurosci. 28, 4861–4871.

Sareen, D., Ebert, A.D., Heins, B.M., McGivern, J.V., Ornelas, L., Svendsen, C.N., 2012. Inhibition of apoptosis blocks human motor neuron cell death in a stem cell model of spinal muscular atrophy. PLoS One 7, e39113.

Schneider, C.A., Rasband, W.S., Eliceiri, K.W., 2012. NIH image to ImageJ: 25 years of image analysis. Nat. Methods 9, 671–675.

Schneider, T.J., Fischer, G.M., Donohoe, T.J., Colarusso, T.P., Rothstein, T.L., 1999. A novel gene coding for a Fas apoptosis inhibitory molecule (FAIM) isolated from inducibly Fas-resistant B lymphocytes. J. Exp. Med. 189, 949–956.

Segura, M.F., Sole, C., Pascual, M., Moubarak, R.S., Perez-Garcia, M.J., Gozzelino, R., Iglesias, V., Badiola, N., Bayascas, J.R., Llecha, N., Rodriguez-Alvarez, J., Soriano, E., Yuste, V.J., Comella, J.X., 2007. The long form of Fas apoptotic inhibitory molecule is expressed specifically in neurons and protects them against death receptor-triggered apoptosis. J. Neurosci. 27, 11228–11241.

Sole, C., Dolcet, X., Segura, M.F., Gutierrez, H., Diaz-Meco, M.T., Gozzelino, R., Sanchis, D., Bayascas, J.R., Gallego, C., Moscat, J., Davies, A.M., Comella, J.X., 2004. The death receptor antagonist FAIM promotes neurite outgrowth by a mechanism that depends on ERK and NF-kapp B signaling. J. Cell Biol. 167, 479–492.

Soler, R.M., Dolcet, X., Encinas, M., Egea, J., Bayascas, J.R., Comella, J.X., 1999. Receptors of the glial cell line-derived neurotrophic factor family of neurotrophic factors signal cell survival through the phosphatidylinositol 3-kinase pathway in spinal cord motoneurons. J. Neurosci. 19, 9160–9169.

Soler-Botija, C., Ferrer, I., Gich, I., Baiget, M., Tizzano, E.F., 2002. Neuronal death is enhanced and begins during foetal development in type I spinal muscular atrophy spinal cord. Brain 125, 1624–1634.

Sumner, C.J., 2006. Therapeutics development for spinal muscular atrophy. NeuroRx 3, 235–245.

Talbot, K., Davies, K.E., 2008. Is good housekeeping the key to motor neuron survival? Cell 133, 572–574.

Tisdale, S., Pellizzoni, L., 2015. Disease mechanisms and therapeutic approaches in spinal muscular atrophy. J. Neurosci. 35, 8691–8700.

Tsai, L.K., Tsai, M.S., Ting, C.H., Wang, S.H., Li, H., 2008. Restoring Bcl-x(L) levels benefits a mouse model of spinal muscular atrophy. Neurobiol. Dis. 31, 361–367.

Tsai, M.S., Chiu, Y.T., Wang, S.H., Hsieh-Li, H.M., Lian, W.C., Li, H., 2006. Abolishing Bax-dependent apoptosis shows beneficial effects on spinal muscular atrophy model mice. Mol. Ther. 13, 1149–1155.

Tseng, Y.T., Chen, C.S., Jong, Y.J., Chang, F.R., Lo, Y.C., 2016. Loganin possesses neuroprotective properties, restores SMN protein and activates protein synthesis positive regulator Akt/mTOR in experimental models of spinal muscular atrophy. Pharmacol. Res. 111, 58–75.

Zhang, H., Xing, L., Rossoll, W., Wichterle, H., Singer, R.H., Bassell, G.J., 2006. Multiprotein complexes of the survival of motor neuron protein SMN with Gemins traffic to neuronal processes and growth cones of motor neurons. J. Neurosci. 26, 8622–8632.

Zhang, Z., Lotti, F., Dittmar, K., Younis, I., Wan, L., Kasim, M., Dreyfuss, G., 2008. SMN deficiency causes tissue-specific perturbations in the repertoire of snRNAs and widespread defects in splicing. Cell 133, 585–600.

Zheleznyakova, G.Y., Voisin, S., Kiselev, A.V., Sällman Almén, M., Xavier, M.J., Maretina, M.A., Tishchenko, L.I., Fredriksson, R., Baranov, V.S., Schiöth, H.B., 2013. Genome-wide analysis shows association of epigenetic changes in regulators of Rab and rho GTPases with spinal muscular atrophy severity. Eur. J. Hum. Genet. 21, 988–993.